ChemPubSoc Europe

DOI: 10.1002/cbic.201600227

CHEMBIOCHEM Full Papers

Regio- and Enantioselective Sequential Dehalogenation of *rac*-1,3-Dibromobutane by Haloalkane Dehalogenase LinB

Johannes Gross,[a] Zbyněk Prokop,[b] Dick Janssen,[c] Kurt Faber,[a] and Mélanie Hall*[a]

The hydrolytic dehalogenation of *rac*-1,3-dibromobutane catalyzed by the haloalkane dehalogenase LinB from *Sphingobium japonicum* UT26 proceeds in a sequential fashion: initial formation of intermediate haloalcohols followed by a second hydrolytic step to produce the final diol. Detailed investigation of the course of the reaction revealed favored nucleophilic displacement of the *sec*-halogen in the first hydrolytic event with pronounced *R* enantioselectivity. The second hydrolysis step proceeded with a regioselectivity switch at the primary position, with preference for the *S* enantiomer. Because of complex competition between all eight possible reactions, intermediate haloalcohols formed with moderate to good *ee* ((*S*)-4-bromobutan-2-ol: up to 87%). Similarly, (*S*)-butane-1,3-diol was formed at a maximum *ee* of 35% before full hydrolysis furnished the racemic diol product.

Introduction

Haloalkane dehalogenases (EC 3.8.1.5) are hydrolytic enzymes that convert a broad range of natural and synthetic halogenated compounds (e.g., alkanes, alkenes, cycloalkanes, alcohols, epoxides, carboxylic acids, esters, ethers, amides, and nitriles) by replacing the halogen atom (chloro, bromo, or iodo) with a hydroxyl group.[1] The first haloalkane dehalogenases were discovered in bacteria isolated from contaminated soil, including DhlA from *Xanthobacter autotrophicus* GJ10,[2] DhaA from *Rhodococcus* sp. 13064,[3] and LinB from *Sphingobium japonicum* UT26.[4] Later, haloalkane dehalogenases were identified in diverse organisms, including the symbiotic bacteria *Bradyrhizobium japonicum* USDA110 and *Mesorhizobium loti* MAFF303099,[5] the plant pathogenic bacteria *Agrobacterium tumefaciens* C58,[6] human pathogenic *Mycobacterium tuberculosis* H37Rv,[7] and the sea urchin *Strongylocentrotus purpuratus*.[8] Structurally similar, haloalkane dehalogenases belong to the α/β-hydrolase fold family, and are classified phylogenetically into subfamilies.[9] Although "universal" substrates have been identified, classification according to substrate specificity has been proposed.[10] These enzymes share a catalytic triad (Asp-His-Glu/Asp), and have three key mechanistic features: 1) an Asp residue acts as nucleophile and replaces the halogen atom by an S_N2 mechanism, thus leading to formation of an enzyme–ester intermediate; 2) hydrolysis of the latter by a water molecule activated by a His/acid pair, thereby releasing the corresponding alcohol; 3) a pair of H-bond donor residues (Asn/Trp, Trp/Trp or Trp/Tyr) form a halide binding site, which stabilizes the halide released in the first step.[11]

LinB was identified as an enzyme in the degradation pathway of γ-hexachlorocyclohexane (γ-HCH; "lindane", a potent insecticide) in *S. japonicum* UT26. LinB catalyzes the successive hydrolytic dechlorination of 1,3,4,6-tetrachlorocyclohexa-1,4-diene (1,4-TCDN) resulting in 2,4,5-trichlorocyclohexa-2,5-dien-1-ol (2,4,5-DNOL), following initial dehydrochlorination of γ-HCH by LinA, in two consecutive steps.[4] The enzyme shows catalytic activity with a broad range of substrates, including halogenated alkanes, alkenes, cycloalkanes, alcohols, carboxylic acids, esters, amides, and nitriles.[12] In some cases, LinB is able to catalyze kinetic resolutions because of the exquisite enantioselectivity, as observed for α-bromo-amides and -esters (*E* value >200).[13a] Simpler secondary haloalkanes are accepted, but stereorecognition is poor (maximum *E* value = 16 for 2-bromopentane).[13] Dihalogenated compounds are also converted, with a general preference for α,ω-dihalo-*n*-alkanes.[12a] Terminally and internally halogenated dihaloalkanes are particular substrates, as hydrolysis to the corresponding diols involves competitive attack between *prim*- and *sec*-halogenated positions. In addition to this regio-divergent behavior, enantioselective recognition at the secondary position (in both hydrolysis steps) renders the overall pathway complex. 1,2-Dibromopropane, for instance, was shown to yield 1-bromopropan-2-ol, thus indicating a LinB preference for the secondary brominated atom.[12b] In contrast, DhlA was selective for the primary position in 1,3-dihaloalkanes.[14] Over the years, enantioselective haloalkane dehalogenases have been applied in synthetic schemes, for example, for the preparation of enantiopure building blocks.[13b,15]

[a] J. Gross, Prof. K. Faber, Dr. M. Hall
Department of Chemistry, University of Graz
Heinrichstrasse 28, 8010 Graz (Austria)
E-mail: melanie.hall@uni-graz.at

[b] Prof. Z. Prokop
Department Experimental Biology, Faculty of Science, Masaryk University
Kamenice 5A13, 625 00 Brno (Czech Republic)

[c] Prof. D. Janssen
Biomolecular Sciences and Biotechnology Institute, University of Groningen
Nijenborgh 4, 9747 AG Groningen (NL)

Supporting information for this article can be found under http://dx.doi.org/10.1002/cbic.201600227.

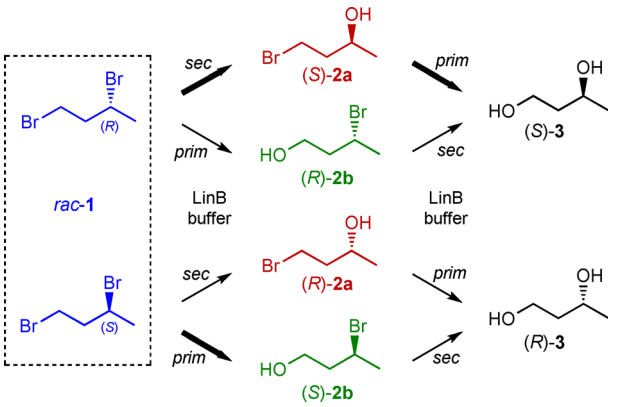

Scheme 1. Sequential dehalogenation of *rac*-**1** catalyzed by haloalkane dehalogenase LinB. Thicker arrows indicate faster reactions.

Thus, LinB-catalyzed hydrolysis of *rac*-1,3-dibromobutane (**1**) was studied, with a focus on the enantio- and regioselective behavior of the enzyme (Scheme 1). Sequential dehalogenation leads to the formation of butane-1,3-diol (**3**), whereas accumulation of haloalcohols **2a** and/or **2b** as intermediates indicates variable selectivity in both hydrolytic steps.

Results and Discussion

The enzymatic hydrolysis of *rac*-1,3-dibromobutane (**1**) to butane-1,3-diol (**3**) follows a complex pathway and involves four possible routes, depending on the regio- and enantioselectivity of the enzyme for the *prim*- or *sec*-halide and the *R* or *S* enantiomer, respectively (Scheme 1). During displacement of the *prim*-halogen, the configuration of the *sec*-halogen is retained (i.e., (*R*)-**1**→(*R*)-**2b** and (*S*)-**1**→(*S*)-**2b**); reaction of the *sec*-halogen atom would proceed with an S_N2-type inversion of the configuration (i.e., (*R*)-**1**→(*S*)-**2a** and (*S*)-**1**→(*R*)-**2a**). Analogous considerations are applicable to the second step, that is, retention for (*S*)-**2a**→(*S*)-**3** and (*R*)-**2a**→(*R*)-**3**, and inversion for (*R*)-**2b**→(*S*)-**3** and (*S*)-**2b**→(*R*)-**3**. Overall, during the first step, kinetic resolution of *rac*-**1** takes place, along with the formation of four products, that is, enantiomeric pairs of the two regioisomeric haloalcohols **2a** and **2b**. In the second step, regioisomers **2a** and **2b** are kinetically resolved to yield one pair of enantiomers of the final hydrolysis product **3**. The enantiomeric compositions of **1**, **2a**, **2b**, and **3** over time depend on the selectivity constants of each step.

Detailed analysis of the course of the reaction was performed by monitoring the composition of the reaction mixture over time, including distribution of regioisomeric haloalcohols **2a** and **2b**. *Rac*-**1** (5 mM) was incubated with lyophilized LinB (6 μM) in Tris·sulfate buffer (50 mM, pH 8.2) at 21 °C with shaking (120 rpm), and samples were withdrawn at intervals. (*S*)-**3** and (*R*)-**3** are commercially available, but both enantiomers of **2a** and **2b** had to be synthesized independently to allow identification of all reaction products (see the Experimental Section).

Careful analysis of the reaction mixture indicated rapid consumption of **1**, with exclusive formation of 4-bromobutan-2-ol

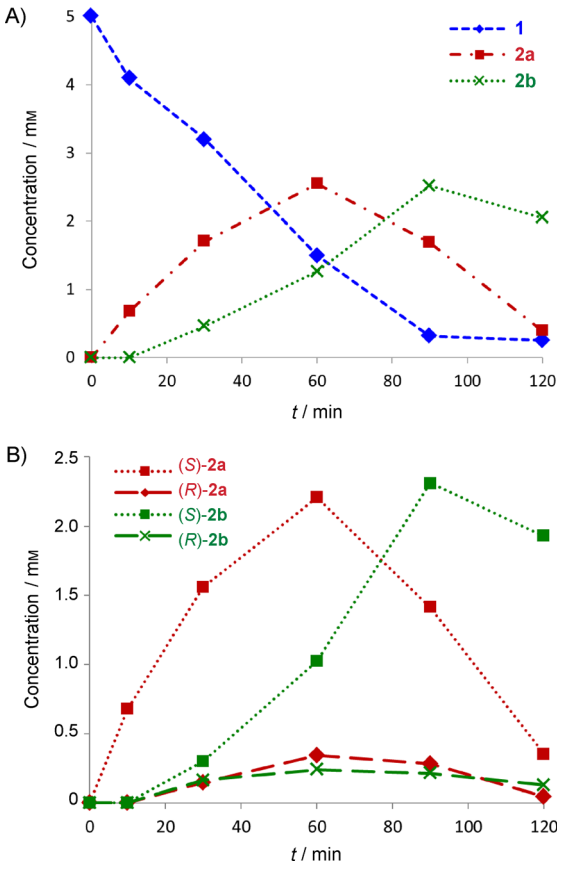

Figure 1. A) Composition of reaction mixture during sequential dehalogenation of *rac*-**1** (5 mM) catalyzed by LinB (values for **3** not plotted due to incomplete recovery; calculated at 120 min from total mass balance: 2.30 mM). B) Enantiomeric composition of **2a** and **2b**.

(**2a**) during the first 10 min, thus highlighting a strong preference for replacement of the *sec*-halogen atom[12b] in the first step of the sequential dehalogenation (Figure 1 A). Gradually, formation of 3-bromobutan-1-ol (**2b**) was observed in the first 60 min, but at a rate which stayed below that for **2a** (Table S1 in the Supporting Information, entries 1–2), thus confirming LinB regioselectivity for the secondary position. After 60 min, the concentration of **2a** began to decrease due to hydrolysis at the primary halogen position, while **2b** continued to accumulate. A slow decline in **2b** concentration due to hydrolysis at the secondary position started to occur only after 90 min, while the hydrolysis rate of **2a** further increased (Table S1, entry 1), thus highlighting a preference for the primary position in the hydrolysis of these haloalcohols. It is noteworthy that all velocity data in Table S1 are apparent values, as both secondary and primary hydrolysis reactions occur simultaneously at some point (e.g., **1** to **2a** or **2b** and **2a** or **2b** to **3**).

In terms of enantiomer distribution, it appeared that the two regiocomplementary hydrolytic reactions with *rac*-**1** have opposite enantiopreference: (*S*)-**2a** accumulated as predominant enantiomer from *sec*-hydrolysis of (*R*)-**1**, whereas (*S*)-**2b** was the major enantiomer in the *prim*-hydrolysis of (*S*)-**1** (Figure 1 B). The concentrations of (*R*)-**2a** and (*R*)-**2b** remained low (< 0.4 mM), and the reaction rates were lowest for these two

enantiomers (Table S1, entries 5–6). Surprisingly, similar reaction velocities were observed for the formation of **2a** and **2b** between 30 and 60 min (Table S1, entries 3 and 6: 0.028 and 0.027 μmol min^{-1} respectively). The delayed hydrolysis of **2b** is likely responsible for the highest rate constant in the whole pathway for the formation of (*S*)-**2b** (0.043 μmol min^{-1} between 60 and 90 min), as **2a** is already being further hydrolyzed.

Taken together, these data explain the *ee* profiles observed over time (Figure 2): the faster reaction of (*R*)-**1** (at the secondary position in the initial step) leads to higher *ee* values for (*S*)-**1**, whereas the *ee* value for (*S*)-**2b** increases (after a lag phase) when its formation is accelerated by faster *prim*-hydrolysis of (*S*)-**1** (this indicates possible inhibition of hydrolysis of (*S*)-**1** by (*R*)-**1**). This pattern is most likely attributable to differences in affinity rather than rate constants, and further studies will be conducted to elucidate the role of each step on the overall pathway. The *ee* value of (*S*)-**2b** remains high because of the overall low reactivity of (*R*)-**1** at the primary position. In the second step of the sequential dehalogenation, **2a** is hydrolyzed, and highest rate of degradation is for (*S*)-**2a**, thus indicating a conserved *S* enantiopreference in the replacement of the *prim*-halogen, as seen for the hydrolysis of *rac*-**1** to (*S*)-**2b**. This appears to be the main reason for the transient accumulation of (*S*)-**3** (maximum 35% *ee*; data not shown).

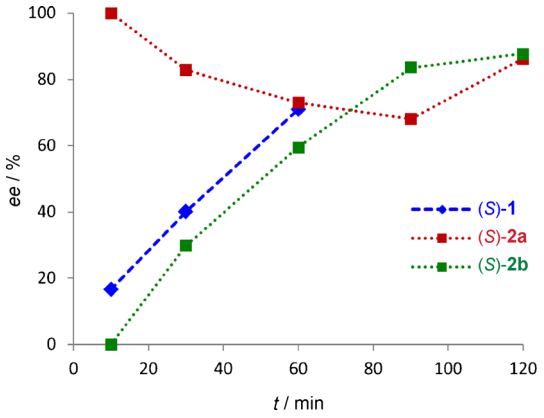

Figure 2. Time profile of *ee* values of **1**, **2a**, and **2b** during LinB catalyzed-dehalogenation of *rac*-**1** (values for (*S*)-**1** calculated from total mass balance, enantiomers not separable).

Eventually, all reactions achieve completion, and *rac*-**1** delivers 100% *rac*-**3**. Because of competition in replacement between the primary and secondary halogen atoms and the complex enantioselective behavior of LinB in both steps of the sequential dehalogenation, the *ee* value of (*S*)-**2a** could be maintained at a reasonable level (>65%) during the major part of the process, whereas (*S*)-**2b** reached 87% *ee* at high accumulated concentration (~2 mM).

Conclusion

Analysis of the sequential dehalogenation of *rac*-1,3-dibromobutane (*rac*-**1**) to butane-1,3-diol (**3**) by LinB via intermediate haloalcohols **2a** and **2b** gave detailed insight into the complex selectivity behavior of LinB in the replacement of primary and secondary halogen atoms as well as enantiorecognition of all isomers formed. Pronounced regiopreference for the *sec*-halogen atom in the first hydrolysis step with significant enantioselectivity led to initial accumulation of (*S*)-**2a**, while regioisomeric (*S*)-**2b** formed more slowly. A regioselectivity switch from *sec*- to *prim*-halogen in the second hydrolysis step was responsible for faster conversion of (*S*)-**2a** compared to (*S*)-**2b**. Enantiopreference in the replacement of *prim*-halogen atom of (*S*)-**1** and (*S*)-**2a** was conserved, regardless of the substitution at the γ-position.

Snapshots obtained at different time points of the reaction indicate that full hydrolysis does not occur from a lack of enantioselectivity, but rather from two regiospecific pathways with relatively high reaction rates. This clearly sets LinB apart from DhlA. Shutting down one of the four predominant pathways could be sufficient to obtain the diol product in a highly enantiopure form, but this calls for challenging protein engineering. Reaction engineering techniques, on the other hand, might afford the isolation of haloalcohols with high *ee* values.

Experimental Section

General: All chemicals, substrates and reference materials were from Sigma–Aldrich, Fluka, and Lancaster Synthesis and used without purification. All solvents were purchased from Roth. Anhydrous solvents were dried over a 4 Å molecular sieve. Anhydrous THF was distilled over sodium/benzophenone. LinB was prepared as reported previously,[16] and was dissolved (10 mg mL^{-1}) in phosphate buffer (50 mM, pH 7.5) and lyophilized for use in further reactions. All biotransformations and rehydration of enzyme preparation were performed at 21 °C in Eppendorf tubes (2 mL) mounted horizontally on a Unitron AJ 260 shaker (120 rpm; HT Infors, Bottmingen, Switzerland). Centrifugation was performed in a Heraeus Biofuge pico (Thermo Fisher Scientific) at 13000 rpm at room temperature.

NMR spectra were recorded in $CDCl_3$ with TMS (0.03%) as the standard on a Bruker NMR device at 300 MHz. Chemical shifts are reported in ppm, and coupling constants are in Hz. GC-MS analysis was on a 7890A GC-System (Agilent Technologies) coupled to a 5975C inert XLMSD detector with an HP-5 MS column (phenylmethylsiloxane (5%), 30 m×0.25 mm×0.25 μm; J&W Scientific/Agilent Technologies). GC-FID measurements on a chiral stationary phase were carried out on the 7890A GC-system with a Hydrodex β-TBDAc column (50 m×0.25 mm i.d.×0.4 mm o.d., Macherey–Nagel). Details are in the Supporting Information. TLC analysis was on silica gel 60 F254 (Merck Millipore). Cerium ammonium molybdate/H_2SO_4 was used as the spray reagent.

General biotransformation procedure: In 2 mL Eppendorf vials, *rac*-**1** (0.6 μL, 5 mM) was added to Tris·sulfate (1 mL, 50 mM, pH 8.2) followed by LinB (125 μL of a 1.5 mg mL^{-1} stock solution; final 6 μM), and the solution was incubated with shaking (120 rpm) for 6 h at 21 °C. The reaction was stopped by saturating the solution with NaCl and adding ethyl acetate (500 μL). The preparation was mixed and centrifuged (13000 rpm, 5 min), and the products were extracted. After a second extraction, the combined organic layers were dried over Na_2SO_4 and transferred into GC glass vials for analysis. Product concentrations were calculated based on GC calibration curves generated for each intermediate available as au-

thentic references (see below). Analytical methods are described in the Supporting Information.

Synthesis of reference materials: Haloalcohol (*R*)-**2b** was obtained in a three-step procedure: 1) protection of the *prim*-OH group of (*S*)-**3** with trityl chloride to yield (*S*)-**4**; 2) Appel reaction by inversion of the configuration to furnish (*R*)-**5;** 3) final deprotection under acidic conditions to yield (*R*)-**2b** (overall yield, 51%). Enantiomer (*S*)-**2b** was prepared by the same procedure starting from (*R*)-**3** (overall yield, 54%). (*R*)-**2a** was prepared in two steps: 1) activation of the *prim*-OH group of (*R*)-**3** with tosyl chloride to yield (*R*)-**6;** 2) nucleophilic substitution using LiBr to furnish (*R*)-**2a** (overall yield, 24%). The same protocol with (*S*)-**3** yielded (*S*)-**2a** (overall yield, 22%). Product identity and purity were confirmed by NMR on **2a** and **2b** at the end of each synthetic sequence.

(*R*)- and (*S*)-4-(Triphenylmethoxy)butan-2-ol ((*R*)- and (*S*)-4):[17] (*R*)-**3** or (*S*)-**3** (180 mg, 2 mmol) in pyridine (350 μL) was added to trityl chloride (631 mg, 2.2 mmol, 1.1 equiv) in pyridine (1.75 mL). DMAP (6 mg, 0.004 mmol) was added, and the mixture was stirred for 48 h at room temperature. After addition of water (5 mL, 0 °C), the residue was extracted with dichloromethane (3×10 mL), dried over Na_2SO_4, and purified by chromatography on silica gel with hexane/ethyl acetate (2:1) to yield (*R*)-**4** (614 mg, 92%) or (*S*)-**4** (570 mg, 85%).

(*R*)- and (*S*)-[(3-Bromobutoxy)methanetrityl]tribenzene ((*R*)- and (*S*)-5):[18] Triphenylphosphine (Ph_3P; 493 mg, 1.88 mmol, 1.1 equiv) was added over 30 min to ice-cooled (*S*)-**4** (570 mg, 1.71 mmol) and CBr_4 (623 mg, 1.88 mmol, 1.1 equiv) in CH_2Cl_2 (750 μL) was added. Alternatively, Ph_3P (535 mg, 2.04 mmol, 1.1 equiv) was added over 30 min to ice-cooled (*R*)-**4** (614 mg, 1.85 mmol) and CBr_4 (670 mg, 2.02 mmol, 1.1 equiv) in CH_2Cl_2 (800 μL). After 3 h of stirring at room temperature, hexane (10 mL) was added. The white precipitate was filtered off, and the remaining solution was concentrated under reduced pressure. The product was purified by chromatography on silica gel with hexane/ethyl acetate (6:1) to yield (*S*)-**5 or** (*R*)-**5** (650 mg, 95%).

(*R*)- and (*S*)-3-Bromobutan-1-ol ((*R*)- and (*S*)-2b): Protected alcohol (*S*)-**5** ([540 mg, 1.37 mmol) or (*R*)-**5** (650 mg, 1.64 mmol) was dissolved in acetic acid (11 mL) at 50 °C with stirring. Water (1.2 mL) was added, and the cloudy solution became clear after being stirred for 3 h at room temperature. The product was extracted with hexane/ethyl acetate (9:1, 3×10 mL) and purified on silica gel with hexane/ethyl acetate (2:1) to yield (*S*)-**2b** (130 mg, 62%) or (*R*)-**2b** (158 mg, 63%). (*S*)-**2b**: ^{1}H NMR: $\delta = 4.39–4.26$ (m, 1H), 3.85–3.81 (m, 2H), 2.10–1.96 (m, 2H), 1.76 (d, $J = 6.70$ Hz, 3H); ^{13}C NMR: $\delta = 60.87$, 47.99, 43.24, 26.55 ppm. ^{1}H NMR spectra were in accordance with those in ref. [19].

(*R*)- and (*S*)-3-Hydroxybutyl 4-methylbenzenesulfonate ((*R*)- and (*S*)-6):[20] *p*-Toluenesulfonyl chloride (472 mg, 2.48 mmol, 1.1 equiv) was added to (*R*)-**3** or (*S*)-**3** (200 mg, 2.22 mmol) in pyridine (1.5 mL) cooled on ice (0 °C). After stirring for 3 h, the reaction mixture was diluted with water and extracted with diethyl ether (3× 10 mL). The organic layer was washed with saturated $CuSO_4$ and dried over Na_2SO_4. After solvent evaporation under reduced pressure, the product was purified on silica gel with hexane/ethyl acetate (2:1) to yield (*R*)-**6** (305 mg, 56%) or (*S*)-**6** (327 mg, 60%).

(*R*)- and (*S*)-4-Bromobutan-2-ol (2a):[21] Lithium bromide (163 mg, 1.87 mmol, 1.5 equiv) was added to (*R*)-**6** (305 mg, 1.25 mmol) or (*S*)-**6** (327 mg, 1.34 mmol) in dry DMF (600 μL). After stirring at room temperature for 5 h, the reaction mixture was diluted with a small amount of water and extracted with diethyl ether (3× 10 mL). The organic layer was washed with water and brine, dried over Na_2SO_4, and concentrated under reduced pressure. The product was purified on silica gel with hexane/ethyl acetate (1:1) to yield (*R*)-**2a** (74 mg, 39%) or (*S*)-**2a** (82 mg, 40%). (*R*)-**2a**: ^{1}H NMR: $\delta = 4.03–3.99$ (m, 1H), 3.61–3.48 (m, 2H), 2.05–1.92 (m, 2H), 1.65 (s, 1H), 1.26 (d, $J = 6.24$ Hz, 3H); ^{13}C NMR: $\delta = 66.1$, 41.5, 30.4, 23.5 ppm. Both ^{1}H NMR and ^{13}C NMR spectra were in accordance with those in ref. [22].

Assignment of absolute configuration: Co-injection of enzymatic samples with authentic reference materials allowed unambiguous assignment of the absolute configuration for all products. GC methods, retention times, and chromatograms are in the Supporting Information.

Acknowledgements

This work was in part supported by the Czech Ministry of Education, Youth and Sports (CZ.1.05/2.1.00/19.0382 and LO1214) and by Grant Agency of the Czech Republic (GA16–07965S).

Keywords: biocatalysis · enantioselectivity · haloalkane dehalogenase · hydrolysis · LinB · regioselectivity

[1] a) D. B. Janssen, A. Scheper, L. Dijkhuizen, B. Witholt, *Appl. Environ. Microbiol.* **1985**, *49*, 673–677; b) T. Leisinger, R. Bader, *Chimia* **1993**, *47*, 116–121; c) S. Fetzner, F. Lingens, *Microbiol. Rev.* **1994**, *58*, 641–685; d) T. Koudelakova, S. Bidmanova, P. Dvorak, A. Pavelka, R. Chaloupkova, Z. Prokop, J. Damborsky, *Biotechnol. J.* **2013**, *8*, 32–45.

[2] S. Keuning, D. B. Janssen, B. Witholt, *J. Bacteriol.* **1985**, *163*, 635–639.

[3] A. N. Kulakova, M. J. Larkin, L. A. Kulakov, *Microbiology* **1997**, *143*, 109–115.

[4] Y. Nagata, T. Nariya, R. Ohtomo, M. Fukuda, K. Yano, M. Takagi, *J. Bacteriol.* **1993**, *175*, 6403–6410.

[5] T. Kaneko, Y. Nakamura, S. Sato, K. Minamisawa, T. Uchiumi, S. Sasamoto, A. Watanabe, K. Idesawa, M. Iriguchi, K. Kawashima, M. Kohara, M. Matsumoto, S. Shimpo, H. Tsuruoka, T. Wada, M. Yamada, S. Tabata, *DNA Res.* **2002**, *9*, 189–197; Y. Sato, M. Monincová, R. Chaloupková, Z. Prokop, Y. Ohtsubo, K. Minamisawa, M. Tsuda, J. Damborský, Y. Nagata, *Appl. Environ. Microbiol.* **2005**, *71*, 4372–4379.

[6] R. Köhler, A. Brokamp, R. Schwarze, R. H. Reiting, F. R. J. Schmidt, *Curr. Microbiol.* **1998**, *36*, 96–101.

[7] S. T. Cole, R. Brosch, J. Parkhill, T. Garnier, C. Churcher, D. Harris, S. V. Gordon, K. Eiglmeier, S. Gas, C. E. Barry III, F. Tekaia, K. Badcock, D. Basham, D. Brown, T. Chillingworth, R. Connor, R. Davies, K. Devlin, T. Feltwell, S. Gentles, N. et al., *Nature* **1998**, *393*, 537–544.

[8] A. Fortova, E. Sebestova, V. Stepankova, T. Koudelakova, L. Palkova, J. Damborsky, R. Chaloupkova, *Biochimie* **2013**, *95*, 2091–2096.

[9] E. Chovancová, J. Kosinski, J. M. Bujnicki, J. Damborsky, *Proteins Struct. Funct. Bioinf.* **2007**, *67*, 305–316.

[10] T. Koudelakova, E. Chovancova, J. Brezovsky, M. Monincova, A. Fortova, J. Jarkovsky, J. Damborský, *Biochem. J.* **2011**, *435*, 345–354.

[11] Z. Prokop, M. Monincová, R. Chaloupková, M. Klvaňa, Y. Nagata, D. B. Janssen, J. Damborský, *J. Biol. Chem.* **2003**, *278*, 45094–45100.

[12] a) J. Damborský, E. Rorije, A. Jesenská, Y. Nagata, G. Klopman, W. J. G. M. Peijnenburg, *Environ. Toxicol. Chem.* **2001**, *20*, 2681–2689; b) J. Kmunicek, K. Hynková, T. Jedlicka, Y. Nagata, A. Negri, F. Gago, R. C. Wade, J. Damborský, *Biochemistry* **2005**, *44*, 3390–3401.

[13] a) Z. Prokop, Y. Sato, J. Brezovsky, T. Mozga, R. Chaloupkova, T. Koudelakova, P. Jerabek, V. Stepankova, R. Natsume, J. G. E. van Leeuwen, D. B. Janssen, J. Florian, Y. Nagata, T. Senda, J. Damborsky, *Angew. Chem. Int. Ed.* **2010**, *49*, 6111–6115; *Angew. Chem.* **2010**, *122*, 6247–6251; b) A. Westerbeek, W. Szymański, H. J. Wijma, S. J. Marrink, B. L. Feringa, D. B. Janssen, *Adv. Synth. Catal.* **2011**, *353*, 931–944.

[14] R. J. Pieters, J. H. L. Spelberg, R. M. Kellogg, D. B. Janssen, *Tetrahedron Lett.* **2001**, *42*, 469–471.

[15] A. Westerbeek, J. G. E. van Leeuwen, W. Szymański, B. L. Feringa, D. B. Janssen, *Tetrahedron* **2012**, *68*, 7645 – 7650.
[16] Y. Nagata, K. Miyauchi, J. Damborsky, K. Manova, A. Ansorgova, M. Takagi, *Appl. Environ. Microbiol.* **1997**, *63*, 3707 – 3710.
[17] I. Uemura, K. Yamada, K. Sugiura, H. Miyagawa, T. Ueno, *Tetrahedron: Asymmetry* **2001**, *12*, 943 – 947.
[18] T. W. Baughman, J. C. Sworen, K. B. Wagener, *Tetrahedron* **2004**, *60*, 10943 – 10948.
[19] J. Coulomb, V. Certal, M.-H. Larraufie, C. Ollivier, J.-P. Corbet, G. Mignani, L. Fensterbank, E. Lacôte, M. Malacria, *Chem. Eur. J.* **2009**, *15*, 10225 – 10232.
[20] J. Térrcio, B. Ferreira, F. Simonelli, *Tetrahedron* **1990**, *46*, 6311 – 6318.
[21] Y. Nakamura, K. Mori, *Eur. J. Org. Chem.* **1999**, 2175 – 2182.
[22] T. Beuerle, S. Engelhard, C. Bicchi, W. Schwab, *J. Nat. Prod.* **1999**, *62*, 35 – 40.

Manuscript received: April 18, 2016
Accepted article published: May 25, 2016
Final article published: ■■ ▮▮, 0000

*J. Gross, Z. Prokop, D. Janssen, K. Faber, M. Hall**

■■ – ■■

Regio- and Enantioselective Sequential Dehalogenation of *rac*-1,3-Dibromobutane by Haloalkane Dehalogenase LinB

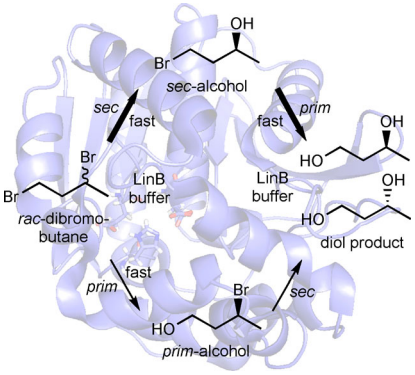

The hydrolytic dehalogenation of *rac*-1,3-dibromobutane catalyzed by the haloalkane dehalogenase LinB proceeds in a sequential fashion via initial intermediate haloalcohols followed by a second hydrolytic step to produce the final diol. Two simultaneous regiospecific pathways with high reaction rates were revealed, along with pronounced enantioselectivity in each pathway.